forests

MDPI

Article

Species and Functional Trait Determinants of Biochar Carbon Retention: Insights from Uniform Smoldering Experiments

Jingyuan Wang

Synthesis Research Center of Chinese Ecosystem Research Network, Key Laboratory of Ecosystem Network Observation and Modeling, Institute of Geographic Sciences and Natural Resources Research, Chinese Academy of Sciences, Beijing 100101, China; wangjy@igsnrr.ac.cn

Abstract

Understanding the influence of tree species and their intrinsic traits on biochar yield and carbon retention is essential for optimizing the conversion of biomass to biochar in carbon-negative systems. While it is well-established that pyrolysis temperature and broad feedstock categories significantly affect biochar properties, the extent of species-level variation within woody biomass under standardized pyrolysis conditions remains insufficiently quantified. Here, we synthesized biochar from seven common subtropical tree species at 600 °C under oxygen-limited smoldering conditions and quantified three key indices: biochar yield (Y), carbon recovery efficiency (ηC), and carbon enrichment factor (EC). We further examined the relationships of these indices with feedstock characteristics (initial carbon content, wood density) and functional group identity (conifer vs. broadleaf). Analysis of variance revealed significant interspecific differences in ηC but weaker effects on Y, indicating that species identity primarily governs carbon retention rather than total mass yield. Broadleaf species (*Liquidambar formosana*, *Castanea mollissima*) exhibited consistently higher ηC and EC than conifers (*Pinus massoniana*, *P. elliottii*), reflecting higher lignin content and wood density that favor aromatic char formation. Principal component and cluster analyses clearly separated coniferous and broadleaf taxa, accounting for over 80% of total variance in carbon-related traits. Regression models showed that feedstock carbon content, biochar carbon content, and wood density together explained 15.5% of the variance in ηC, with feedstock carbon content exerting a significant negative effect, whereas wood density correlated positively with carbon retention. These findings demonstrate that tree species and their functional traits jointly determine carbon fixation efficiency during smoldering. High initial carbon content alone does not guarantee enhanced carbon recovery; instead, wood density and lignin-derived structural stability dominate retention outcomes. Our results underscore the need for trait-based feedstock selection to improve biochar quality and carbon sequestration potential, and provide a mechanistic framework linking species identity, functional traits, and carbon stabilization in biochar production.

Keywords: uniform smolder; biochar; carbon retention; carbon recovery efficiency; carbon enrichment factor

Check for updates

Academic Editors: Donald L. Rockwood and Giovanna Battipaglia

Received: 3 December 2025
Revised: 4 January 2026
Accepted: 13 January 2026
Published: 14 January 2026

Copyright: © 2026 by the author. Licensee MDPI, Basel, Switzerland. This article is an open access article distributed under the terms and conditions of the Creative Commons Attribution (CC BY) license.

1. Introduction

Biochar is a carbon-rich solid produced by pyrolyzing biomass under oxygen-limited conditions. Because of its stability and porosity, biochar is widely used to improve soils and sequester carbon over the long-term [1,2]. Biochar properties (e.g., C content, H/C and O/C ratios, surface chemistry, and pore structure) and their effects on soils depend

strongly on feedstock and pyrolysis conditions (temperature, residence time, and heating rate) [3]. These factors create trade-offs among solid, liquid, and gas yields and the stability of the retained carbon [4,5]. Higher pyrolysis temperatures usually reduce solid yield but increase aromaticity and carbon stability [6].

Feedstocks (woody biomass, herbaceous plants, crop and forestry residues, and manures) differ in composition (lignin, cellulose, hemicellulose), ash and mineral catalysts, and anatomical structure [7–9]. These differences shape the biochar carbon content, yield, and functional groups [10,11]. For example, feedstock and temperature jointly determine the biochar C content, pH, inorganic composition, and yield. At the component level, char formation often follows lignin > hemicellulose > cellulose; thus, lignin-rich feedstocks usually yield more char and more aromatic structures [12]. Ash and inorganic phases can catalyze reactions and nucleate carbon structures, affecting yield and carbon partitioning [13].

Across biomass sources, biochar shows large differences in pH, ash content, nutrient levels, and specific surface area [14,15]. For example, Evans et al. (2017) reported acidic pine sawdust biochar (pH 4.6) but strongly alkaline Miscanthus biochar (pH 9.3) [16]. Ash content strongly influences biochar yield and final ash fraction; crop residues such as rice and wheat straw often contain more ash [17,18]. Manure-derived biochars are often rich in P, K, Ca, and Mg [16], whereas residue-derived biochars can contain substantial water-soluble K [19]. Specific surface area also varies by feedstock: Liao et al. (2018) reported that herbaceous biochar generally present relatively low surface areas (2–70 $m^2\ g^{-1}$), whereas woody biochar can reach much higher values (200–380 $m^2\ g^{-1}$) [20].

Despite extensive cross-feedstock research, species-level differences within woody biomass under standardized pyrolysis remain poorly quantified. Most studies use two-factor designs (feedstock class × temperature) and pay less attention to how species identity and traits (e.g., wood density, anatomy, extractives, ash, and lignin composition) jointly shape yield, carbon recovery efficiency, and carbon enrichment [21]. Comparative studies suggest that feedstock type and species shift biochar elemental composition and C content, whereas higher temperatures reduce solid yield [12,22]. Together, these findings motivate tests of functional-group effects (conifer vs. broadleaf) on biochar properties [23].

A trait-based approach can link species identity to biochar characteristics by using measurable indicators such as initial C, lignin, ash, and wood density [6]. Fundamental pyrolysis studies suggest three mechanisms. First, higher lignin increases char residue and aromaticity. Second, ash can redirect decomposition via mineral catalysis and shift yield and carbon allocation. Third, density and anatomy affect heat and mass transfer and oxygen diffusion during smoldering, altering carbon retention [23]. Together, these results suggest that species identity, functional group, and traits jointly explain variation in biochar carbon indices [24].

Building on this background, we quantified biochar yield, carbon recovery efficiency, and carbon enrichment factor for seven common tree species under standardized smoldering. In this study, we decomposed the observed interspecific differences in biochar properties into functional group (conifer vs. broadleaf) and trait-level components to (1) determine whether tree species identity exerts significant effects on biochar yield, carbon recovery efficiency, and carbon enrichment factor; (2) assess whether coniferous and broadleaf species can be differentiated in multivariate trait space and whether broadleaf species exhibit higher carbon recovery efficiencies and/or carbon contents; and (3) identify the key feedstock traits that drive variations in biochar carbon metrics, including the roles of initial carbon content, lignin and ash contents, and wood density. These analyses clarify how species identity, functional groups, and traits govern carbon retention and transformation during smoldering, thereby advancing our understanding of species-level mechanisms underlying biochar formation and carbon sequestration potential.

We tested three hypotheses for interspecific variation in biochar carbon retention under standardized smoldering. (1) Functional group identity would structure biochar carbon metrics: because broadleaved species (e.g., *Liquidambar formosana* and *Castanea mollissima*) typically exhibit higher lignin contents and wood densities than conifers (e.g., *Pinus massoniana* and *P. elliottii*), broadleaves were predicted to show significantly higher carbon recovery efficiency (ηC) and carbon enrichment factor (E_C) than conifers. (2) Negative association between feedstock initial carbon content and (ηC), such that higher initial C does not necessarily translate into greater carbon sequestration potential, consistent with the possibility that C-rich tissues contain larger pools of thermally labile constituents that are preferentially lost as gaseous products during conversion. (3) Intrinsic structural traits are primary determinants of carbon retention, with physical and chemical attributes linked to structural stability—particularly wood density and lignin-mediated recalcitrance—exerting stronger effects on (ηC) and (E_C) than on total mass yield (Y).

2. Materials and Methods

2.1. Study Site

The study was conducted at the Qianyanzhou Subtropical Forest Ecosystem Research Station (26°44′29″ N, 115°03′29″ E; 102 m elevation), a core site of the Chinese Ecosystem Research Network (CERN) (Figure 1). The region is a typical red-soil hilly area under a subtropical monsoon climate, with prevailing northwesterly winds in winter and southeasterly winds in summer. The planted forests are approximately 30 years old and dominated by *Pinus massoniana*, *Cunninghamia lanceolata*, and *Pinus elliottii*, with an average canopy height of about 12 m. The understory shrub layer includes *Adinandra millettii* and *Vaccinium sprengelii*, while the herb layer is dominated by ferns such as *Woodwardia japonica*, *Dicranopteris dichotoma*, and *Dryopteris atrata*. Overall vegetation cover exceeds 90%.

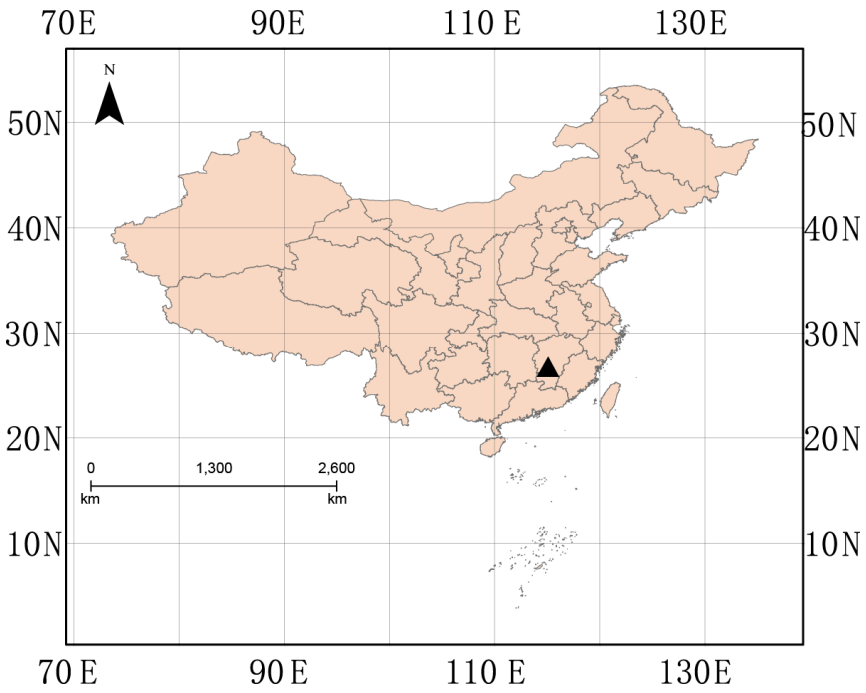


Figure 1. Locations of study sites (indicated by the triangle). QYZ, Qianyanzhou.

2.2. Biochar Production and Feedstock

Biochar was produced from stem wood of seven tree species collected at the study site. All samples were air-dried, cut into standardized stem segments, and then pyrolyzed at 600 °C under oxygen-limited conditions. Heating was carried out in a con-

trolled smoldering/slow pyrolysis system to minimize variability in temperature and residence time among samples (600 °C, 8 h). Basic biochar properties for each species are summarized in Table 1.

Table 1. Species composition and sample sizes.

Species	Functional Group	n
Castanea mollissima	Broadleaf	5
Cinnamomum camphora	Broadleaf	9
Cunninghamia lanceolata	Coniferous	5
Liquidambar formosana	Broadleaf	11
Pinus elliottii	Coniferous	10
Pinus massoniana	Coniferous	32
Triadica sebifera	Broadleaf	23

2.3. Calculation of Carbon Indices

Biochar yield (Y) was defined as the proportion of dry feedstock mass converted to biochar residue after pyrolysis:

$$Y = \frac{m_{biochar}}{m_{feedstock}} \times 100\%$$

where $m_{biochar}$ is the dry mass of biochar (g) and $m_{feedstock}$ is the dry mass of the original feedstock (g). Yield reflects the degree of carbonization and mass loss; it typically decreases with increasing pyrolysis temperature due to enhanced release of volatiles.

Carbon recovery efficiency (ηC) quantifies the fraction of initial carbon retained in the biochar:

$$\eta C = \frac{m_{biochar} \times C_{biochar}}{m_{feedstock} \times C_{feedstock}} \times 100\%$$

where $C_{biochar}$ and $C_{feedstock}$ are carbon mass fractions (%) in biochar and feedstock, respectively. This index integrates both yield and carbon content, thus reflects the "retention capacity" of carbon during pyrolysis.

The carbon enrichment factor (E_C) describes the degree of carbon concentration in biochar relative to the feedstock:

$$E_C = \frac{C_{biochar}}{C_{feedstock}}$$

with $E_C > 1$ indicating carbon enrichment, $E_C = 1$ denoting no net change (theoretical), and $E_C < 1$ suggesting carbon dilution or potential analytical artifacts.

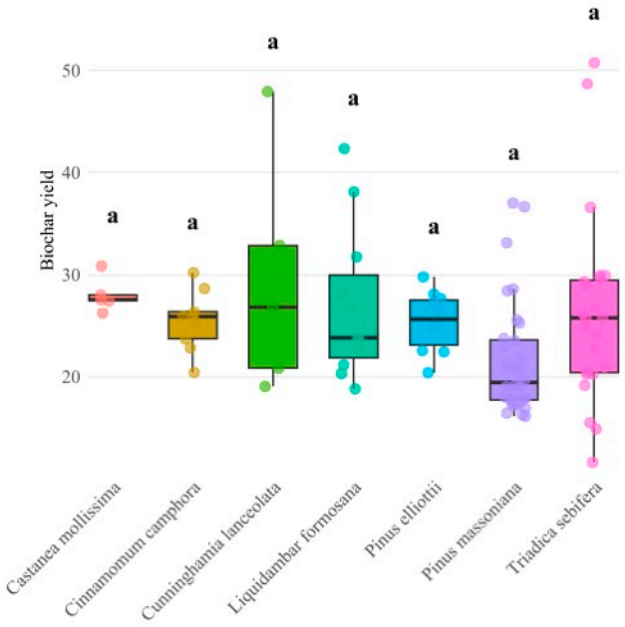
2.4. Statistical Analyses

All statistical analyses were conducted in R (v4.5.1). Tree species were treated as a categorical factor. Species differences in biochar yield, carbon recovery efficiency, and carbon enrichment factor were tested using one-way ANOVA, followed by Tukey HSD post hoc grouping implemented with agricolae::HSD.test (v1.3-7). Results were visualized as ggplot2 (v4.0.0) boxplots annotated with grouping letters. To summarize multivariate patterns across biochar properties and feedstock traits, principal component analysis (PCA) was performed using FactoMineR::PCA (v2.12) with scale.unit = TRUE (Z-standardization). PCA was conducted primarily on species-level means, with an additional PCA on individual observations to visualize within-species dispersion; ordinations were plotted with factoextra/ggplot2 (v1.0.7) and key outputs (scores, loadings, contributions) were exported.

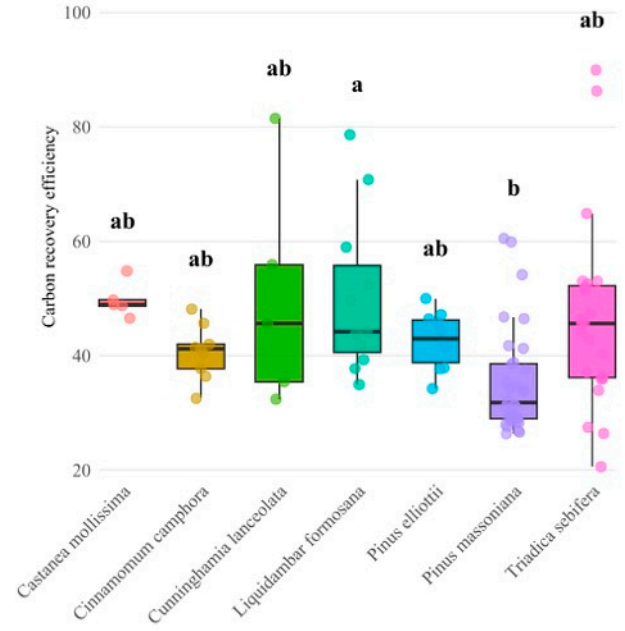
3. Results

3.1. Species Effects: Stronger Influence on Carbon Recovery Efficiency than on Yield

Under standardized smoldering conditions, tree species identity marginally affected carbon recovery efficiency, while its effect on yield was weaker (Figure 2). One-way ANOVA showed a significant species effect on ηC, and Tukey post-hoc tests grouped several species into distinct significance classes. In contrast, species differences in Y were less pronounced, with overall tests either not reaching statistical significance or only marginally significant.

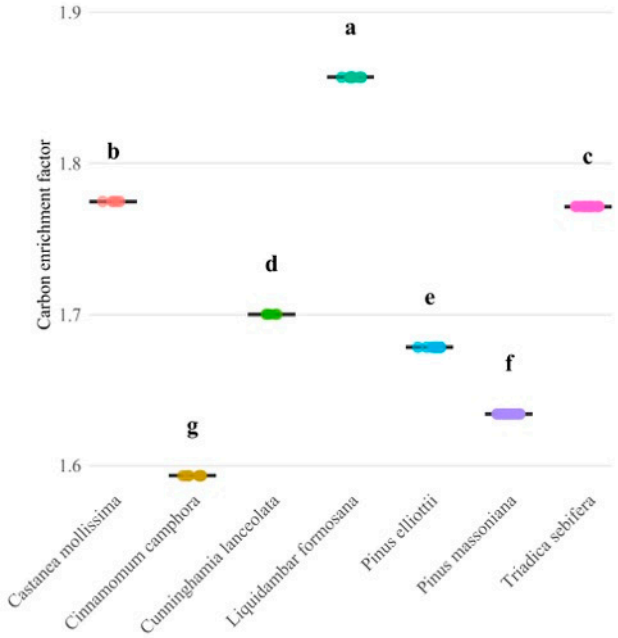


(**a**)



(**b**)

Figure 2. *Cont.*



(**c**)

Figure 2. Biochar production characteristics of seven tree species under uniform smoldering conditions. Panels show the (**a**) biochar yield, (**b**) carbon recovery efficiency, and (**c**) carbon enrichment factor. Data are presented as mean ± standard deviation, different lowercase letters above bars indicate significant differences among species (Tukey's HSD, $p < 0.05$).

In terms of mean patterns, *Cunninghamia lanceolata*, *Liquidambar formosana*, and *Castanea mollissima* exhibited relatively high carbon recovery efficiencies, while *Pinus massoniana* and *P. elliottii* showed lower values; *Triadica sebifera* and *Cinnamomum camphora* tended to fall in the intermediate range. Notably, *Liquidambar formosana* had the highest median ηC, which was significantly higher than that of *P. massoniana. Pinus massoniana* had the lowest median and a broad distribution range, and its ηC was significantly lower than that of several other species. Differences among the remaining species were generally not significant, indicating a cluster of intermediate-efficiency species.

3.2. Functional Group Differences: Conifers and Broadleaves Separate in Multivariate Space

Multivariate analyses revealed a clear separation between coniferous and broadleaf species. In PCA space, the seven species were ordered along PC1, which was primarily associated with carbon recovery efficiency and yield, and PC2, which was associated with material properties approximated by wood density. PC1 and PC2 explained 63.5% and 18.5% of the total variance, respectively, yielding a cumulative variance of 82.0% (Figure 3), indicating that these two axes captured most of the variation in carbon-related traits.

Variable loadings showed that carbon recovery efficiency, biochar yield, and carbon enrichment factor loaded strongly and negatively on PC1, indicating a tight positive association among these indices and defining a primary axis of carbon accumulation and use efficiency. Biochar carbon content and initial feedstock carbon content contributed mainly to PC2, representing a gradient of carbon concentration and structural attributes. Wood density displayed modest and more neutral loadings, suggesting a limited direct role in separating species along a single PCA axis.

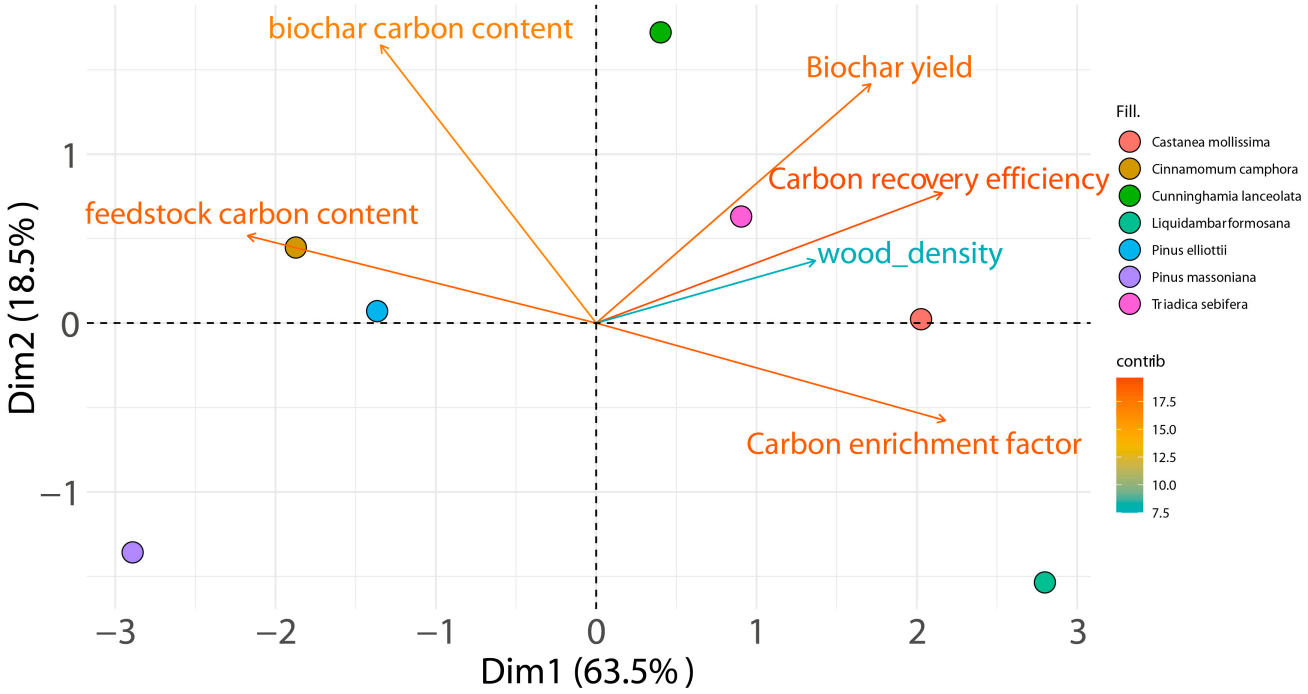


Figure 3. Principal component analysis (PCA) of biochar characteristics derived from seven tree species under uniform smoldering conditions.

Species scores revealed distinct positions in PCA space: *Liquidambar formosana* and *Castanea mollissima* plotted on the positive side of PC1, corresponding to high ηC and relatively high yields and enrichment factors, and can thus be considered high carbon-accumulation species. *Pinus massoniana* occupied the negative region of PC1, indicative of comparatively low carbon recovery efficiency. *Cunninghamia lanceolata* and *Triadica sebifera* were located in the upper-right region, with relatively high ηC and moderate yields. *P. elliottii* and *Cinnamomum camphora* fell in intermediate positions. High $\cos^2$ values for *Liquidambar formosana*, *Castanea mollissima*, and *P. massoniana* indicated that these species were particularly well represented by the first two principal components.

Hierarchical clustering (Ward.D2, Euclidean distance) further grouped *P. elliottii* and *P. massoniana* into one clade and *C. lanceolata*, *Liquidambar formosana*, and *Castanea mollissima* into another, with *Triadica sebifera* and *Cinnamomum camphora* forming intermediate branches. This pattern is consistent with the conifer–broadleaf functional group distinction: conifers (especially *Pinus elliottii and P. massoniana*) are characterized by lower density, lower ash content, and higher volatile fractions, typically leading to reduced yield and carbon recovery, whereas broadleaves (e.g., *Liquidambar formosana*, *Castanea mollissima*) possess higher lignin contents and denser tissues, which favor the formation of aromatic, carbon-rich solids under identical conditions.

3.3. Trait-Driven Patterns: Correlations Present, but Regression Models Have Limited Explanatory Power

Correlation analyses showed a strong positive relationship between yield and carbon recovery efficiency, reflecting their shared dependence on carbon retention during pyrolysis. Initial feedstock carbon content correlated negatively with both yield and ηC, and the carbon enrichment factor correlated negatively with feedstock carbon content. The latter pattern is partly a mathematical consequence of the definition of EC as the ratio of biochar carbon content to feedstock carbon content, particularly when variation in the numerator is relatively small.

Multiple regression models indicated that feedstock carbon content, biochar carbon content, and wood density together explained 6.5% of the variation in yield, with the overall model not significant at $\alpha = 0.05$ ($p \approx 0.10$) (Table 2). In contrast, the same set of predictors explained 15.5% of the variation in carbon recovery efficiency, with the overall model highly significant ($p \approx 0.0015$). Among individual predictors, only feedstock carbon content had a significantly negative coefficient ($p \approx 0.02$), whereas the coefficients for biochar carbon content and wood density did not reach statistical significance. Wood density showed a positive correlation with ηC and the enrichment factor, consistent with the notion that dense woods are more likely to form highly aromatic and stable chars [25].

Table 2. Multiple linear regression results for biochar yield and carbon recovery efficiency.

	Biochar Yield	**Carbon Recovery Efficiency**
(Intercept)	37.583 (40.070)	115.646 (69.449)
'Feedstock carbon content'	−0.567 (0.441)	−1.809 * (0.764)
'biochar carbon content'	0.160 (0.568)	0.167 (0.984)
Wood density	5.386 (7.810)	9.252 (13.537)
R^2	0.065	0.155
Adj. R^2	0.034	0.127
Num. obs.	95	95

Note. * $p < 0.05$.

4. Discussion

Results demonstrate that under standardized smoldering conditions, tree species identity primarily modifies the efficiency of carbon retention (feedstock carbon converted to solid carbon) rather than overall mass yield, which is more susceptible to experimental variability and subtle differences in operating conditions. This pattern—where carbon recovery efficiency is more sensitive than yield—is consistent with the conceptual framework describing a trade-off between yield and aromatic stability during pyrolysis [24]. Species differ in lignin, cellulose, hemicellulose, and ash, which shifts decomposition pathways and char formation and ultimately changes the fraction of carbon retained [13]. Syntheses consistently identify feedstock composition as a primary determinant of biochar properties and carbon retention, especially when temperature varies little [6,23].

Across-species studies have reported higher carbon recovery efficiencies for hardwoods than for softwoods, and this pattern was consistent with the present findings [26–28]. These differences are commonly attributed to higher lignin content, slower degradation rates, and denser structural frameworks in hardwoods, which jointly promote the formation and persistence of aromatic carbon. Furthermore, studies that compare conifer- and broadleaf-derived biochar have shown higher aromatic carbon contents and lower oxidation degrees in broadleaf biochar, implying greater long-term stability [29,30]. Microstructural analyses indicate that conifer-derived chars tend to be more porous and less dense, which is less favorable for long-term carbon retention [31,32]. The functional group contrast observed here—higher ηC in broadleaf species relative to conifers—is therefore consistent with known differences in density, ash content, and lignin proportion.

A strong positive correlation between yield and carbon recovery efficiency was also observed, consistent with previous work in which coordinated responses of yield and carbon retention to feedstock structure and pyrolysis conditions have been documented [13]. However, the negative relationship between initial feedstock carbon content and both yield and ηC suggests that high-carbon feedstocks do not necessarily translate into higher carbon retention. This agrees with modeling and machine-learning studies suggesting greater gas-phase losses from some C-rich feedstocks at high temperatures [33].

The negative correlation between carbon enrichment factor and feedstock carbon content is partly mathematical, because EC is defined as a ratio; when variation in biochar carbon content is relatively constrained, higher feedstock carbon content reduces the ratio value [34]. In our regression analyses, feedstock carbon content, biochar carbon content, and wood density explained only 6.5% of the variance in yield, indicating that yield is predominantly controlled by process parameters such as temperature profile and residence time rather than by a small set of chemical traits. In contrast, the same predictors explained 15.5% of ηC, with feedstock carbon content exerting a significant negative effect. The positive association between wood density and ηC is consistent with reports that denser woods form more aromatic, thermally stable chars [14,25].

Taken together, our results support the notion that high initial feedstock carbon content does not guarantee high carbon recovery efficiency [35,36]. Instead, structural traits and thermal stability—largely governed by lignin content, density, and mineral composition—play a dominant role in determining carbon fixation during pyrolysis [37]. These insights provide a mechanistic basis for selecting woody feedstocks for high-efficiency biochar production within carbon-negative strategies. They also emphasize that functional groups (e.g., “conifer” vs. “broadleaf”) should be treated as statistical aggregates of underlying trait distributions rather than mechanistic units. Therefore, trait-based selection may transfer better across systems than category-based selection [38,39].

More broadly, our findings are consistent with fundamental pyrolysis chemistry: the typical hierarchy of char yields (lignin > hemicellulose > cellulose) and the catalytic and nucleation roles of mineral ash jointly modulate decomposition pathways, condensation reactions, and ultimately carbon retention in biochar [14,24]. By analyzing species identity, functional groups, and traits under identical conditions, this study links woody feedstocks to biochar carbon metrics and supports trait-based optimization for carbon management.

5. Conclusions

This study highlights that under uniform smoldering, woody species identity altered carbon recovery efficiency more strongly than biochar yield, indicating that feedstock-specific pathways govern carbon retention beyond simple mass conversion. In multivariate space, broadleaves occupied the high-efficiency/high-enrichment region, whereas *Pinus elliottii* and *Pinus massoniana* clustered at low efficiency, consistent with clear functional-group separation along PC axes capturing most variation. Although yield covaried tightly with carbon recovery efficiency and feedstock carbon content was negatively associated with both, a minimal trait set (feedstock C, biochar C, wood density) explained little of yield variance and only modest variance in ηC, implying additional control by unmeasured chemistry and fine-scale process heterogeneity. Overall, these findings support trait-based feedstock selection for carbon-negative biochar strategies, treating functional groups as useful summaries rather than mechanistic units.

Funding: This research was funded by the Natural Science Foundation of China (Grant No. 32371559).

Data Availability Statement: The data presented in this study are available on request from the author on reasonable request.

Acknowledgments: The author gratefully acknowledge the support and assistance of the Qianyanzhou Subtropical Forest Ecosystem Research Station, Chinese Academy of Sciences in enabling this research work.

Conflicts of Interest: The author declares no conflicts of interest.

References

1. Murillo-Acevedo, Y.; Grande, C. Grass clippings to biochar: A promising soil amendment for sustainable agriculture under drip irrigation. *J. Environ. Chem. Eng.* **2024**, *12*, 114856. [CrossRef]
2. Zhang, C.; Liu, N.; Zhang, T.; Su, S.; Li, R.; Feng, J.; Wu, Y. Influence of biomass type and pyrolysis temperature on biochar characteristics for enhanced soil amendment. *J. Anal. Appl. Pyrolysis* **2025**, *192*, 107257. [CrossRef]
3. Spokas, K.A. Review of the stability of biochar in soils: Predictability of O:C molar ratios. *Carbon Manag.* **2014**, *1*, 289–303. [CrossRef]
4. Ma, Z.; Wang, Q.; Wang, X.; Chen, X.; Wang, Y.; Mao, Z. Effects of Biochar on Replant Disease by Amendment Soil Environment. *Commun. Soil Sci. Plant Anal.* **2021**, *52*, 673–685. [CrossRef]
5. Prodana, M.; Bastos, A.; Silva, A.; Morgado, R.; Frankenbach, S.; Serôdio, J.; Soares, A.; Loureiro, S. Soil functional assessment under biochar, organic amendments and fertilizers applications in small-scale terrestrial ecosystem models. *Appl. Soil Ecol.* **2021**, *168*, 104157. [CrossRef]
6. Lehmann, J.; Joseph, S. *Biochar for Environmental Management Science, Technology and Implementation*; Routledge: London, UK, 2015.
7. Zhou, H.; Guo, J.; Liu, H.; Wang, J.; Wang, Y. Effects of Biochar Pyrolysis Temperature and Application Rate on Saline Soil Quality and Maize Yield. *Agronomy* **2024**, *14*, 1529. [CrossRef]
8. Wu, Z.; Fan, Y.; Zhou, Z.; Hao, X.; Kang, S. Interaction between biochar particle size and soil salinity levels on soil properties and tomato yield. *Biochar* **2025**, *7*, 30. [CrossRef]
9. Zhu, Z.; Zhang, Y.; Tao, W.; Zhang, X.; Xu, Z.; Xu, C. The Biological Effects of Biochar on Soil's Physical and Chemical Characteristics: A Review. *Sustainability* **2025**, *17*, 2214. [CrossRef]
10. Gani, A.; Naruse, I. Effect of cellulose and lignin content on pyrolysis and combustion characteristics for several types of biomass. *Renew. Energy* **2007**, *32*, 649–661. [CrossRef]
11. Anand, A.; Gautam, S.; Ram, L. Feedstock and pyrolysis conditions affect suitability of biochar for various sustainable energy and environmental applications. *J. Anal. Appl. Pyrolysis* **2023**, *170*, 105881. [CrossRef]
12. Zhang, X.; Zhang, P.; Yuan, X.; Li, Y.; Han, L. Effect of pyrolysis temperature and correlation analysis on the yield and physicochemical properties of crop residue biochar. *Bioresour. Technol.* **2020**, *296*, 122318. [CrossRef]
13. Enders, A.; Hanley, K.; Whitman, T.; Joseph, S.; Lehmann, J. Characterization of biochars to evaluate recalcitrance and agronomic performance. *Bioresour. Technol.* **2012**, *114*, 644–653. [CrossRef] [PubMed]
14. Li, W.; Dang, Q.; Brown, R.C.; Laird, D.; Wright, M.M. The impacts of biomass properties on pyrolysis yields, economic and environmental performance of the pyrolysis-bioenergy-biochar platform to carbon negative energy. *Bioresour. Technol.* **2017**, *241*, 959–968. [CrossRef]
15. Li, L.; Long, A.; Fossum, B.; Kaiser, M. Effects of pyrolysis temperature and feedstock type on biochar characteristics pertinent to soil carbon and soil health: A meta-analysis. *Soil Use Manag.* **2022**, *39*, 43–52. [CrossRef]
16. Evans, M.; Jackson, B.; Popp, M.; Sadaka, S. Chemical Properties of Biochar Materials Manufactured from Agricultural Products Common to the Southeast United States. *Horttechnology* **2017**, *27*, 16–23. [CrossRef]
17. Keiluweit, M.; Kleber, M.; Sparrow, M.; Simoneit, B.; Prahl, F. Solvent-Extractable Polycyclic Aromatic Hydrocarbons in Biochar: Influence of Pyrolysis Temperature and Feedstock. *Environ. Sci. Technol.* **2012**, *46*, 9333–9341. [CrossRef] [PubMed]
18. Allen, J.; Downie, A. Predicting Slow Pyrolysis Process Outcomes with Simplified Empirical Correlations for a Consistent Higher Heating Temperature: Biochar Yield and Ash Content. *Energy Fuels* **2020**, *34*, 14223–14231. [CrossRef]
19. Bera, T.; Purakayastha, T.; Patra, A.; Datta, S. Comparative analysis of physicochemical, nutrient, and spectral properties of agricultural residue biochars as influenced by pyrolysis temperatures. *J. Mater. Cycles Waste Manag.* **2018**, *20*, 1115–1127. [CrossRef]
20. Liao, F.; Yang, L.; Li, Q.; Li, Y.; Yang, L.; Anas, M.; Huang, D. Characteristics and inorganic N holding ability of biochar derived from the pyrolysis of agricultural and forestal residues in the southern China. *J. Anal. Appl. Pyrolysis* **2018**, *134*, 544–551. [CrossRef]
21. Anand, A.; Gautam, S.; Ram, L. A characteristic-based decision tree approach for sustainable energy applications of biomass residues from two major classes. *Fuel* **2023**, *339*, 127483. [CrossRef]
22. Lataf, A.; Jozefczak, M.; Vandecasteele, B.; Viaene, J.; Schreurs, S.; Carleer, R.; Yperman, J.; Marchal, W.; Cuypers, A.; Vandamme, D. The effect of pyrolysis temperature and feedstock on biochar agronomic properties. *J. Anal. Appl. Pyrolysis* **2022**, *168*, 105728. [CrossRef]

23. Kloss, S.; Zehetner, F.; Dellantonio, A.; Hamid, R.; Ottner, F.; Liedtke, V.; Schwanninger, M.; Gerzabek, M.H.; Soja, G. Characterization of slow pyrolysis biochars: Effects of feedstocks and pyrolysis temperature on biochar properties. *J. Environ. Qual.* **2012**, *41*, 990–1000. [CrossRef]
24. Chen, D.; Cen, K.; Zhuang, X.; Gan, Z.; Zhou, J.; Zhang, Y.; Zhang, H. Insight into biomass pyrolysis mechanism based on cellulose, hemicellulose, and lignin: Evolution of volatiles and kinetics, elucidation of reaction pathways, and characterization of gas, biochar and bio-oil. *Combust. Flame* **2022**, *242*, 112142. [CrossRef]
25. Crombie, K.; Mašek, O.; Sohi, S.P.; Brownsort, P.; Cross, A. The effect of pyrolysis conditions on biochar stability as determined by three methods. *GCB Bioenergy* **2012**, *5*, 122–131. [CrossRef]
26. Grojzdek, M.; Novosel, B.; Klinar, D.; Golob, J.; Žgajnar Gotvajn, A. Pyrolysis of different wood species: Influence of process conditions on biochar properties and gas-phase composition. *Biomass Convers. Biorefin.* **2021**, *14*, 6027–6037. [CrossRef]
27. Anderson, N.; Jones, J.; Page-Dumroese, D.; McCollum, D.; Baker, S.; Loeffler, D.; Chung, W. A Comparison of Producer Gas, Biochar, and Activated Carbon from Two Distributed Scale Thermochemical Conversion Systems Used to Process Forest Biomass. *Energies* **2013**, *6*, 164–183. [CrossRef]
28. Lekaviciene, K.; Jotautiene, E.; Grigas, A.; Gaudutis, A.; Paulikiene, S.; Mieldazys, R. Evaluating biochar extraction from waste tree stumps in different pyrolysis systems using life cycle analysis. *Sci. Rep.* **2025**, *15*, 40135. [CrossRef]
29. Thomas, S.; Gale, N. Biochar and forest restoration: A review and meta-analysis of tree growth responses. *New For.* **2015**, *46*, 931–946. [CrossRef]
30. Ohtsuka, T.; Tomotsune, M.; Ando, M.; Tsukimori, Y.; Koizumi, H.; Yoshitake, S. Effects of the Application of Biochar to Plant Growth and Net Primary Production in an Oak Forest. *Forests* **2021**, *12*, 152. [CrossRef]
31. Hagemann, N.; Schmidt, H.P.; Kagi, R.; Bohler, M.; Sigmund, G.; Maccagnan, A.; McArdell, C.S.; Bucheli, T.D. Wood-based activated biochar to eliminate organic micropollutants from biologically treated wastewater. *Sci. Total Environ.* **2020**, *730*, 138417. [CrossRef]
32. Korus, A.; Samson, A.; Szlęk, A. Catalytic conversion of toluene over a biochar bed under an inert atmosphere—The comparison of chars from different types of wood and the role of selected metals. *Fuel* **2020**, *279*, 118458. [CrossRef]
33. Zhu, J.; Jin, L.; Li, J.; Bao, Z.; Li, Y.; Hu, H. Fast pyrolysis behaviors of cedar in an infrared-heated fixed-bed reactor. *Bioresour. Technol.* **2019**, *290*, 121739. [CrossRef]
34. Batista, R.R.; Gomes, M.M. Effects of Chemical Composition and Pyrolysis Process Variables on Biochar Yields: Correlation and Principal Component Analysis. *Floresta Ambiente* **2021**, *28*, e20210007. [CrossRef]
35. Wan, J.; Liu, L.; Wang, G.; Sang, L.; Liang, W.; Zhang, W.; Peng, C.; Fu, R. Unveiling the mechanisms of carbon conversion and loss in biochars derived from characteristic lignocellulosic biomass. *J. Environ. Chem. Eng.* **2022**, *10*, 108403. [CrossRef]
36. Shahbaz, M.; AlNouss, A.; Parthasarathy, P.; Abdelaal, A.H.; Mackey, H.; McKay, G.; Al-Ansari, T. Investigation of biomass components on the slow pyrolysis products yield using Aspen Plus for techno-economic analysis. *Biomass Convers. Biorefin.* **2020**, *12*, 669–681. [CrossRef]
37. Chun, D.D.; Ni, D.; Simson, A. The effect of inherent inorganics and CO_2 co-pyrolysis on biochar production from biowastes and their gasification reactivity. *Biomass Bioenergy* **2022**, *158*, 106361. [CrossRef]
38. Singh, B.P.; Cowie, A.L.; Smernik, R.J. Biochar carbon stability in a clayey soil as a function of feedstock and pyrolysis temperature. *Environ. Sci. Technol.* **2012**, *46*, 11770–11778. [CrossRef] [PubMed]
39. Akhil, D.; Lakshmi, D.; Kartik, A.; Vo, D.V.; Arun, J.; Gopinath, K.P. Production, characterization, activation and environmental applications of engineered biochar: A review. *Environ. Chem. Lett.* **2021**, *19*, 2261–2297. [CrossRef]

Disclaimer/Publisher's Note: The statements, opinions and data contained in all publications are solely those of the individual author(s) and contributor(s) and not of MDPI and/or the editor(s). MDPI and/or the editor(s) disclaim responsibility for any injury to people or property resulting from any ideas, methods, instructions or products referred to in the content.